Supplemental Materials

Molecular Biology of the Cell

Phillips-Krawczak et al.

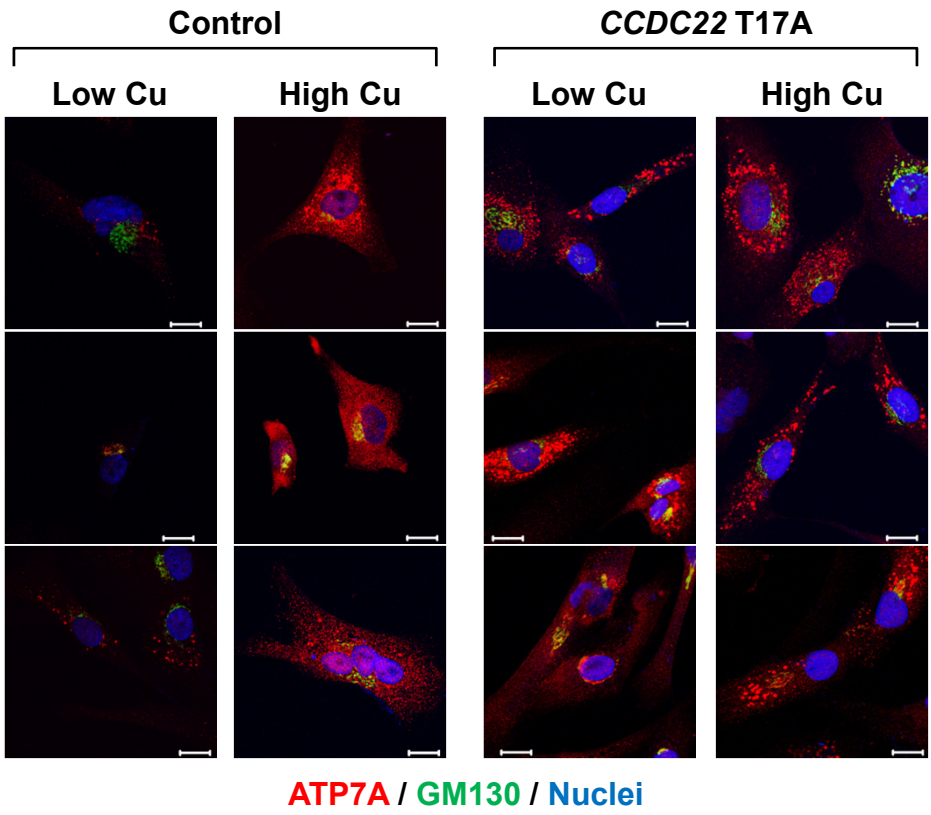

Figure S1. Role of CCDC22 in ATP7A localization. ATP7A localization in response to copper treatment was evaluated in control and *CCDC22* T17A mutant fibroblasts. Scale bar = 20 μm.

A

Gene		Identity (%)	
Species	Symbol	Protein	DNA
H.sapiens	**CCDC22**		
vs. P.troglodytes	CCDC22	100.0	99.6
vs. M.mulatta	CCDC22	98.4	98.1
vs. C.lupus	CCDC22	91.5	89.6
vs. B.taurus	CCDC22	90.9	90.1
vs. M.musculus	Ccdc22	88.0	85.7
vs. R.norvegicus	Ccdc22	87.9	85.7
vs. D.rerio	ccdc22	58.0	61.1
vs. D.melanogaster	CG9951	30.6	44.9
vs. A.gambiae	CCDC22_ANOGA	38.8	51.0
vs. A.thaliana	AT1G55830	34.0	44.3

B

Gene		Identity (%)	
Species	Symbol	Protein	DNA
H.sapiens	**CCDC93**		
vs. M.mulatta	LOC694513	98.8	98.5
vs. C.lupus	CCDC93	95.4	91.9
vs. B.taurus	CCDC93	93.8	90.4
vs. M.musculus	Ccdc93	92.1	86.8
vs. R.norvegicus	Ccdc93	93.0	86.7
vs. G.gallus	CCDC93	80.8	75.3
vs. D.rerio	ccdc93	70.9	67.6
vs. D.melanogaster	fidipidine	41.7	50.2
vs. A.gambiae	AgaP_AGAP009044	44.4	52.9
vs. C.elegans	C16A11.2	24.3	39.3
vs. A.thaliana	AT4G32560	30.4	44.5

C

Gene		Identity (%)	
Species	Symbol	Protein	DNA
H.sapiens	**C16orf62**		
vs. P.troglodytes	C16H16orf62	98.8	98.9
vs. M.mulatta	LOC695027	98.1	97.5
vs. C.lupus	C6H16orf62	96.6	92.0
vs. B.taurus	C25H16orf62	96.9	91.9
vs. M.musculus	9030624J02Rik	92.3	86.2
vs. R.norvegicus	LOC361635	93.7	87.6
vs. G.gallus	C14H16orf62	86.3	77.1
vs. D.rerio	zgc:163107	74.0	69.2
vs. D.melanogaster	CG8202	44.7	52.1
vs. A.gambiae	AgaP_AGAP001150	48.9	53.5
vs. C.elegans	CELE_F26G1.1	24.1	39.0
vs. A.thaliana	AT1G50730	25.5	42.6

Figure S2. Conservation of CCC complex components. (A-C). Protein and DNA sequence identity from various organisms compiled from NCBI HomoloGene Pairwise Alignment Scores. CCDC22, CCDC93 and C16orf62 are displayed.

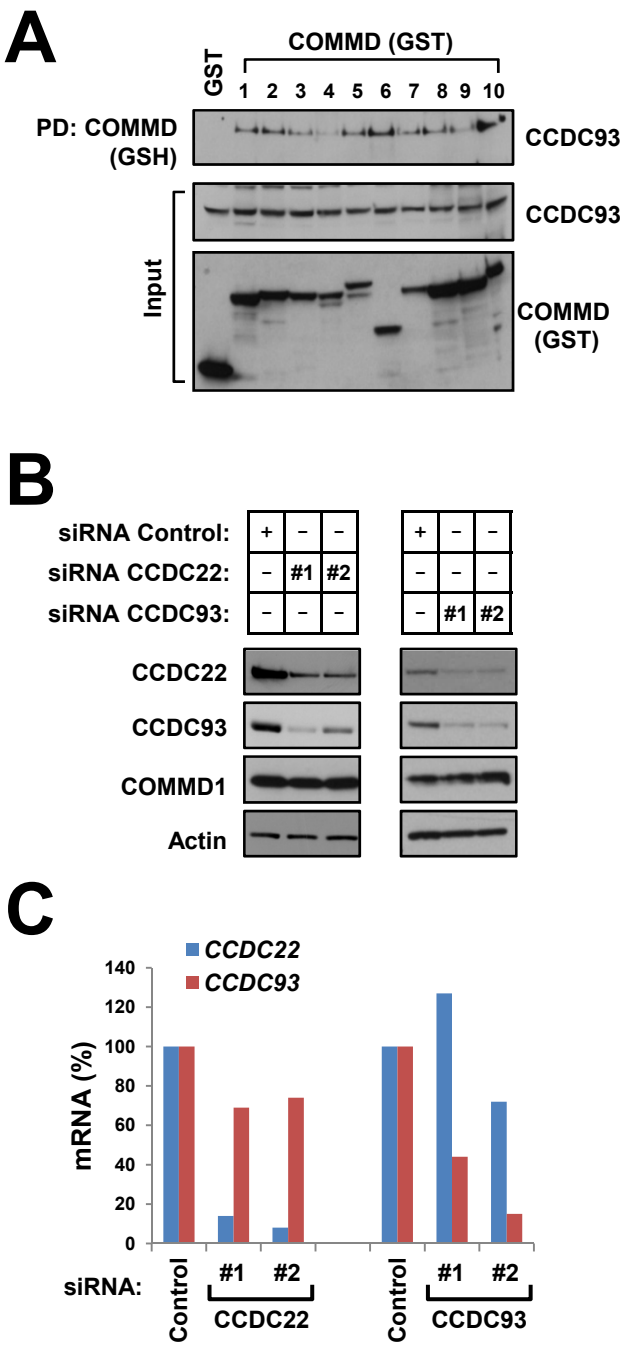

Figure S3. CCC complex shows interdependency for complex stability. (A) Binding to CCDC93 was evaluated by expressing COMMD proteins fused to GST in HEK293T cells. The proteins were subsequently precipitated from Triton X-100 lysates and the recovered material was immunoblotted for endogenous CCDC93 or GST. PD, pulldown. **(B, C)** Protein and RNA was isolated from HeLa cells transfected with either control siRNA or siRNA toward CCDC22 or CCDC93. Subsequently, western blot analysis (B) and qRT-PCR (C) was performed to determine the effect on CCDC22 and CCDC93 expression.

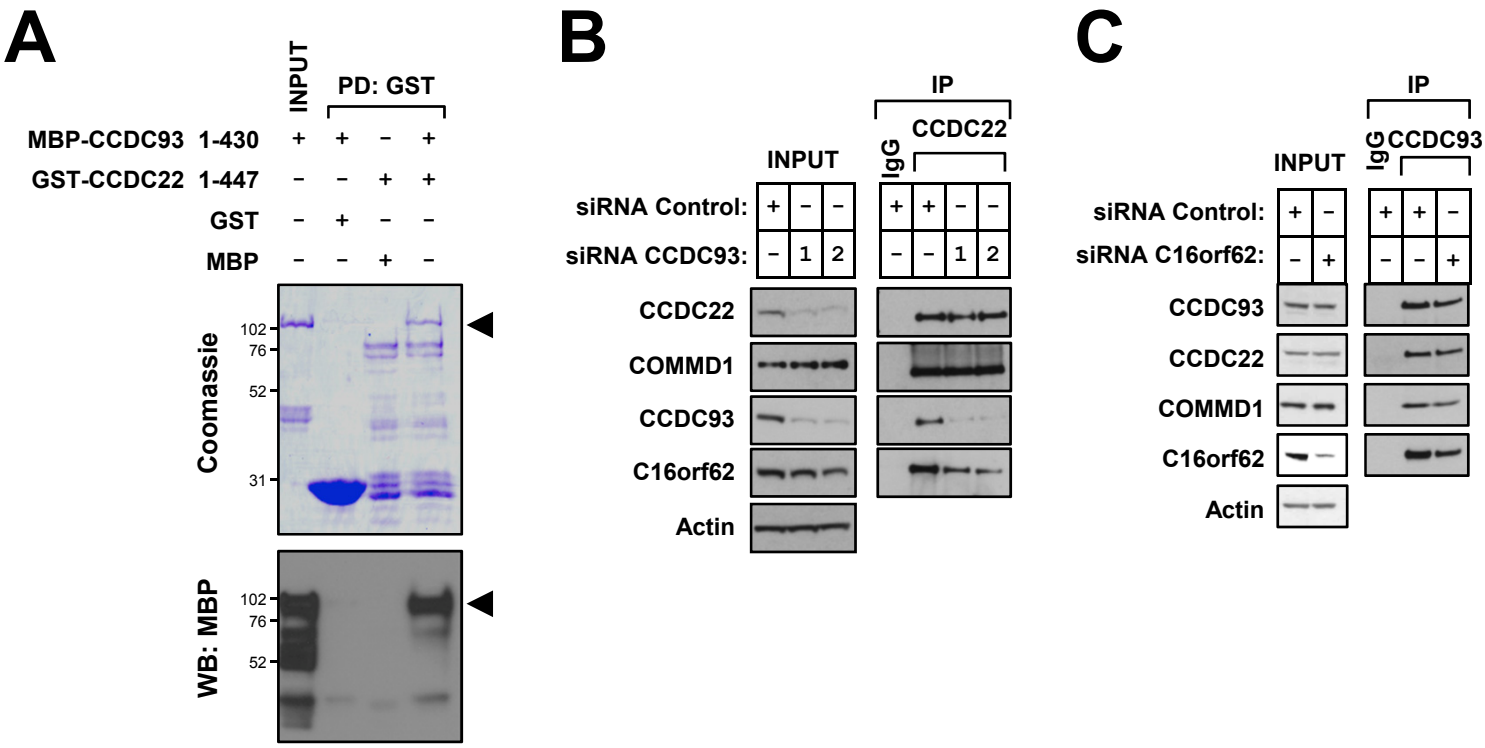

Figure S4. Interactions that mediate CCC complex assembly. (A) *In vitro* interactions between *E. coli* generated recombinant CCDC22 and CCDC93 fragments was assessed. After precipitation of GST-CCDC22, the presence of co-precipitated MBP-CCDC93 was determined by Coomassie staining and by immunoblotting. **(B)** CCDC93 was silenced in HEK293T cells using two independent siRNA duplexes. Subsequently, CCDC22 was immunoprecipitated and interactions with other CCC components were assessed by immunoblotting. **(C)** C16orf62 was silenced by siRNA in HEK293T cells. Subsequently, CCDC93 was immunoprecipitated and co-precipitated proteins were detected by immunoblotting.

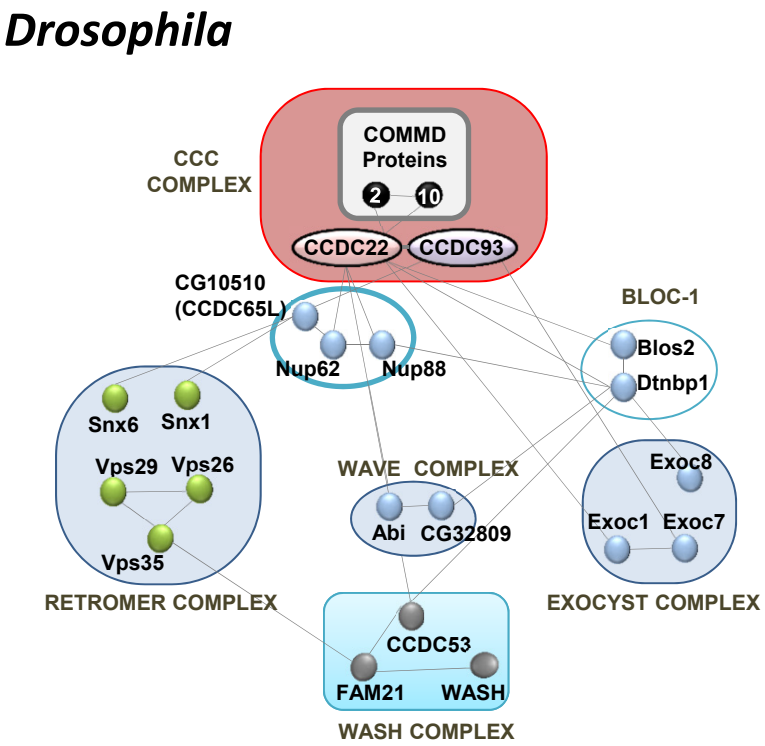

Figure S5. CCC complex Drosophila interaction map. Interaction maps between CCC complex components and other cellular complexes were drawn using data extracted from NCBI. Intra-complex interactions, where useful, were also indicated.

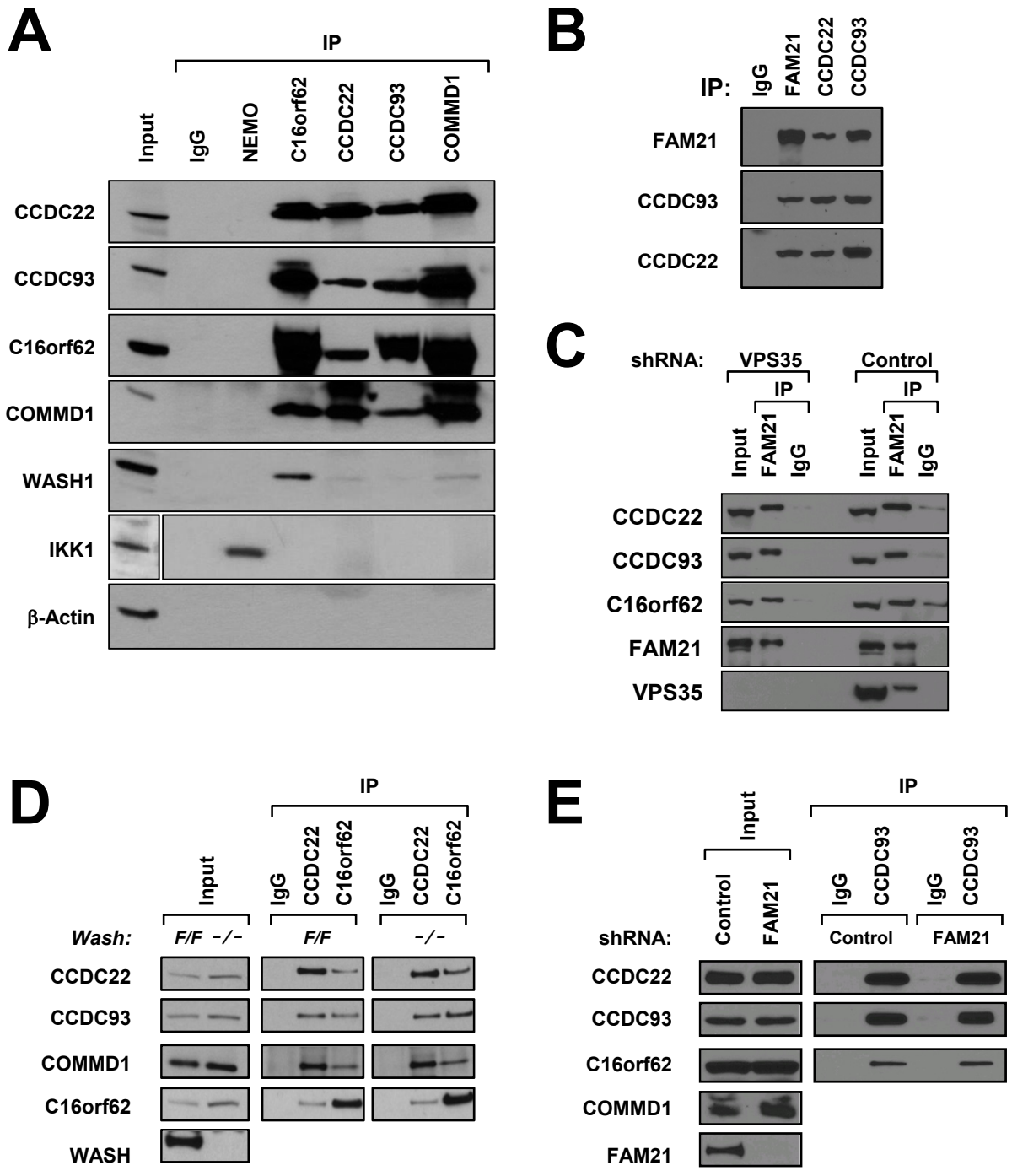

Figure S6. CCC complex interactions do not require retromer or WASH complex. (A) Coprecipitation between CCC complex components, as well as the WASH complex subunit WASH1. The coiled-coil protein NEMO, and it's known interacting partner IKK1, are included as additional controls. **(B)** HeLa cell lysates were immunoprecipitated and immunoblotted as indicated to assess CCC complex interactions with FAM21. **(C,D)** Cell lysates from the indicated cell lines were used for immunoprecipitation and immunoblotting analysis to assess CCC interactions in the absence of retromer **(C,** using HeLa cells expressing shRNA targeting VPS35) or WASH **(D,** using Wash-deficient fibroblasts). **(E)** Interactions between CCDC93 and its partners CCDC22 and C16orf62 were assessed by co-immunoprecipitation in control and FAM21-depleted HeLa cells.

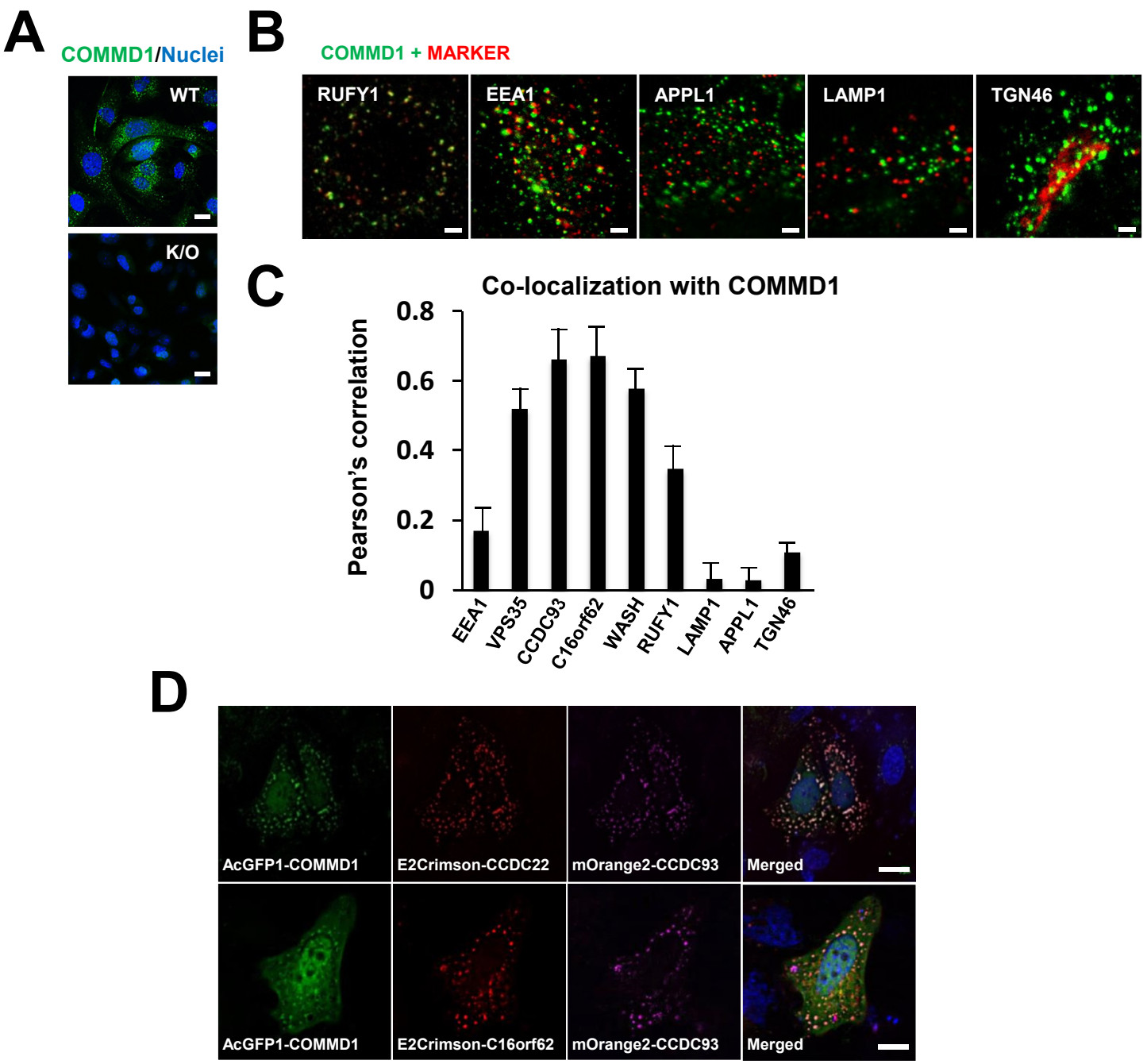

Figure S7. CCC complex localizes to distinct endosomal compartments enriched in WASH and Retromer. (A) Commd1 deficient (*Commd1*$^{-/-}$) and isogenic control fibroblasts were stained for COMMD1 (green) and nuclei (blue) and imaged by confocal microscopy (scale bar of 10 μm). **(B, C)** Co-localization of endogenous COMMD1 (green) and various vesicular markers, as indicated, was assessed by immunofluorescence staining of HeLa cells (scale bar of 5 μm). Representative images are shown (B) and co-localization coefficients were calculated and plotted based on these images as well as those in Figure 3C,D (C). **(D)** Live cell imaging of HeLa cells transiently expressing the indicated fluorescent proteins depicts the co-localization of CCC complex components. Scale bar = 5 μm.

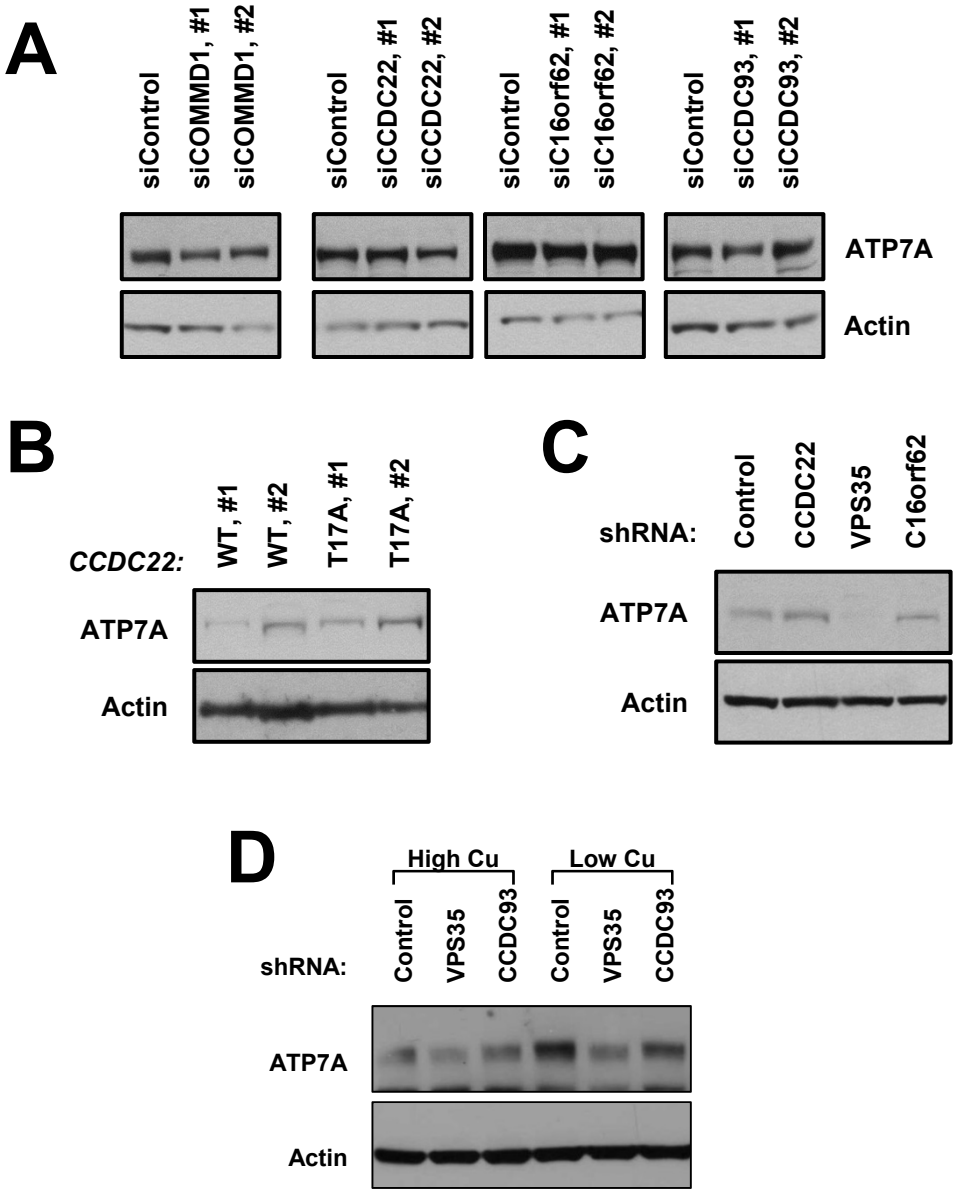

Figure S8. Effects of CCC deficiency on ATP7A protein expression. (A) HeLa cells were transfected with the indicated siRNA oligonucleotides and the expression levels of ATP7A were ascertained by immunoblot. **(B)** ATP7A levels in fibroblasts derived from 2 control individuals (WT) and two patients with the *CCDC22* T17A mutation. **(C)** ATP7A levels in cell lines with stable silencing of the indicated genes. Only VPS35 depletion led to significant effects on ATP7A expression levels. **(D)** ATP7A levels in the indicated cells lines were evaluated under conditions of high and low copper availability in the media.

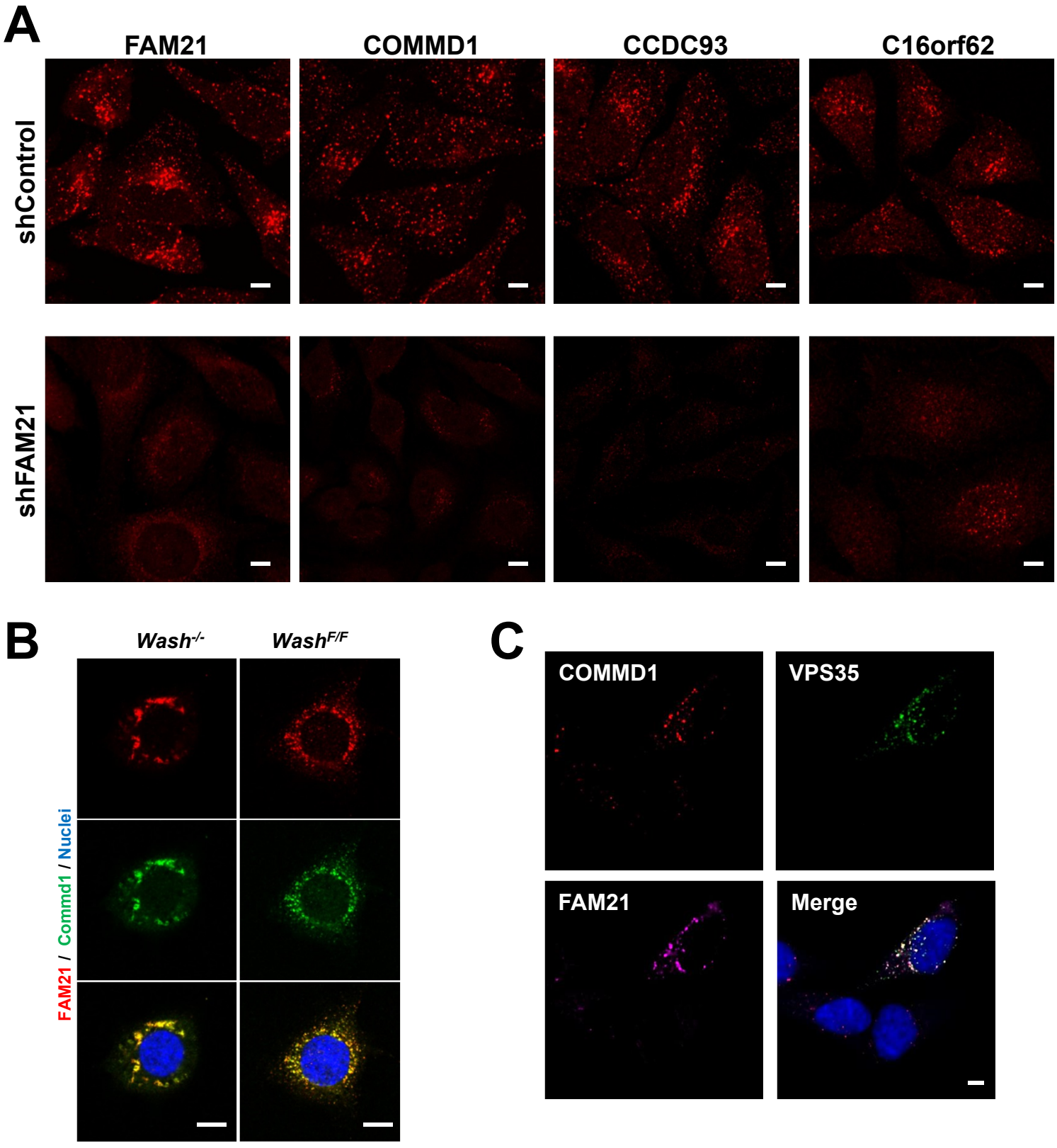

Figure S9. CCC complex localizes to endosomes with FAM21. (A) Enlarged images from Figure 5A showing only staining for the indicated proteins in the control and shFAM21-depleted HeLa cell lines. Scale bar = 5 μm. **(B)** WASH-deficient (*Wash*$^{-/-}$) and isogenic control fibroblasts were stained with anti-COMMD1 antibody (green), anti-FAM21 (red) and nuclei (blue) and imaged by confocal microscopy.Scale bar = 10 μm. **(C)** HeLa scramble control and shVPS35 cells were mixed 1:1, plated on coverslips and stained as indicated. Scale bar = 5 μm.

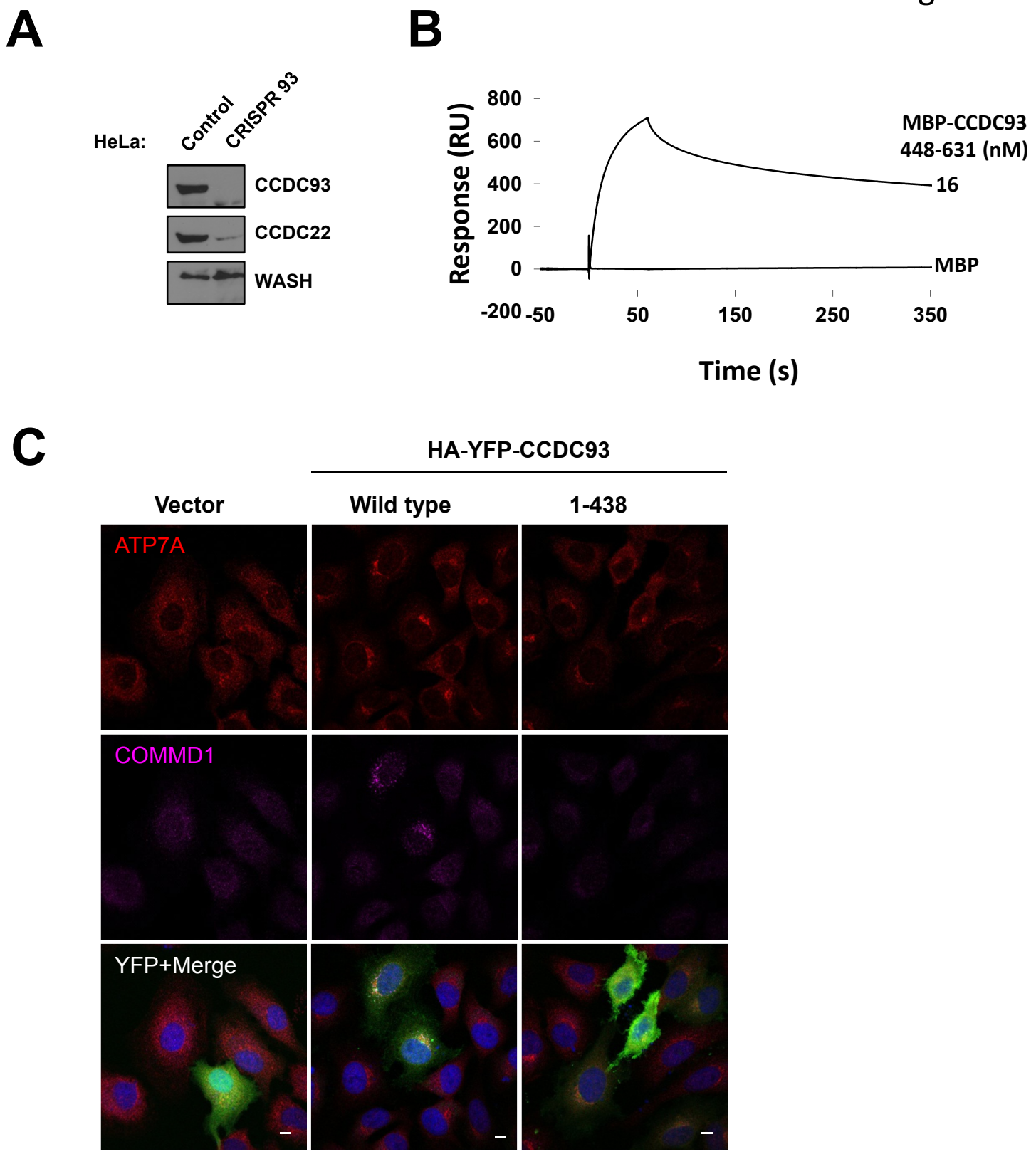

Figure S10. (A) CRISPR/Cas9 mediated deletion of CCDC93 in HeLa cells. Loss of CCDC93 expression is shown by WB, which also demonstrates the concurrent reduction in CCDC22 expression. **(B)** Control SPR experiment. The indicated concentrations of MBP or MBP-CCDC93 were assessed for binding with GST-FAM21-FN using SPR. **(C)** Low magnification images of the CRISPR-93 HeLa line transfected with YFP vector or YFP-CCDC93 wild type or 1-438 mutant and imaged for ATP7A and COMMD1 localization under low copper conditions. Scale bar = 10μm.

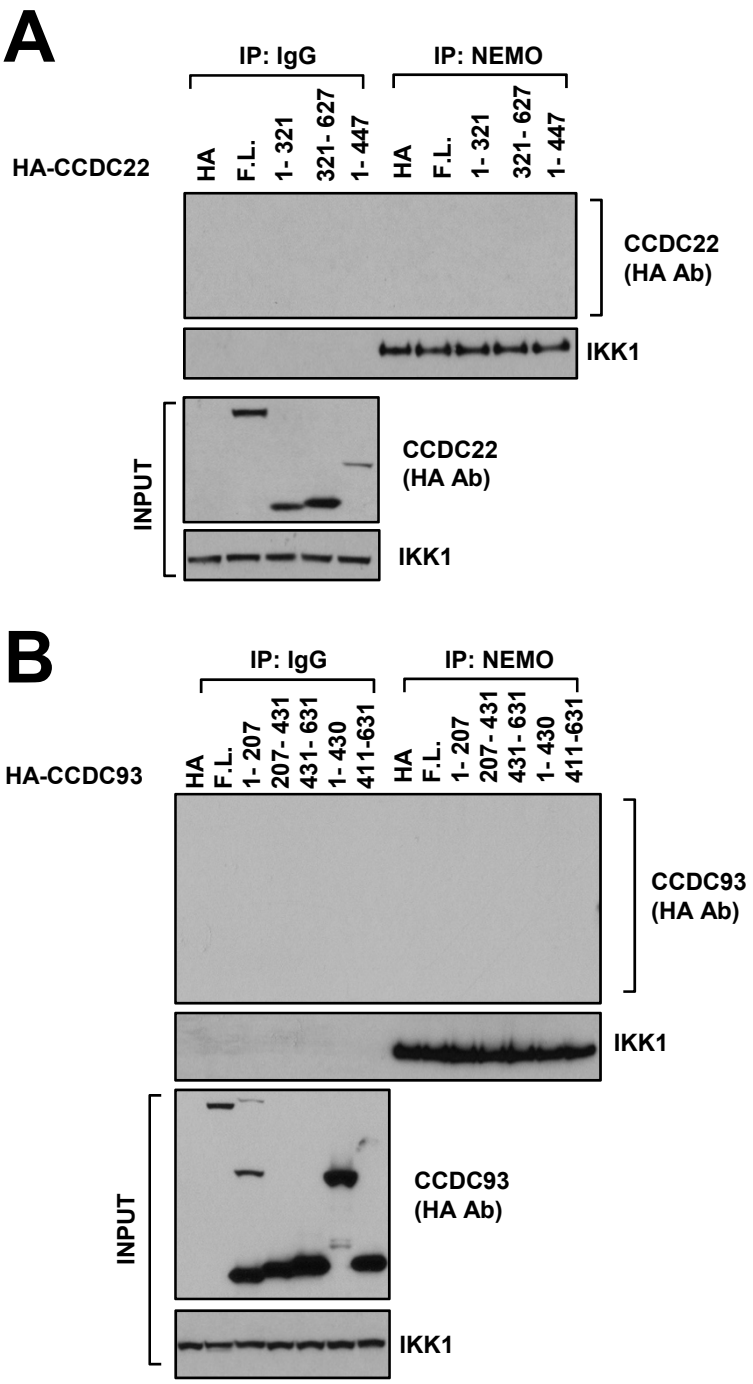

Figure S11. (A, B) The indicated domains of CCDC22 (A) and CCDC93 (B) were expressed in 293 cells. Subsequently, cell lysates were subjected to immunoprecipitation with control IgG or an antibody against NEMO. IKK1 is a known partner of NEMO and serves as a positive control.

Table S1: siRNA and shRNA sequences utilized

siRNA sequences	
Gene target (human)	***Oligo sequence***
CCDC22# 1	CCACUGAGCUGGUUGUAGA
CCDC22 # 2	CCAAGACUGGUGCUCCUAA
CCDC93 # 1	CCGUAUAUCACCUACAAGA
CCDC93# 2	GAUUGUGUCCGAGUAUGCA
C16orf62 # 1	GAGAAAUCCUUGCCCGGUA
C16orf62 # 2	GAUCCUAGAGCAUCUGAAA
shRNA sequences	
Gene target (human)	***shRNA sequence***
CCDC22	GATGAGCTTGTGTTCAAGGAT
CCDC93	GACCTAGACAGACGGTATAAT
C16orf62	GCCTGTTCTTGTGCAGTTGAT
FAM21	CCCCACAGCAAACCTTCTAAA
VPS35	AACAGAGCAGATTAACAAACA

Table S2: Antibodies utilized

Target protein	***Supplier***	***Cat. No.***
GM130	BD Transduction labs	610822
CCDC22	ProteinTech Group	16636-1-AP
CCDC93	ProteinTech Group	20861-1-AP
C16orf62	Pierce	PA5-28553
COMMD1	R & D systems	MAB7526
VPS35	AbCam	ab10099-199
EEA1	BD Biosciences	610456
APPL1	Cell Signaling Technology	3858S
RUFY1	ProteinTech Group	13498-1-AP
LAMP1	AbCam	ab24170
TGN46	Sigma Aldrich	T7576
β-Actin	Sigma Aldrich	A5441
HA	Covance	MMS101R
MBP	Immuno Consultants Lab	RMBP45-A-Z
GST	Santa Cruz	Sc-459
N-cadherin	BD Biosciences	610920

Table S3: Primers utilized for qRT-PCR (human genes)

Target	***Sense primer***	***Antisense primer***
CCDC93	AGGCTTATCACCCTTTGACAAG	GGCAGGACCGAGACAATTTTT
CCDC22	CTATCAGAACTTCCTCTACCC	GGAGAATAGCTGAGTCACCT
ACTB	GCGGGAAATCGTGCGTGACATT	GATGGAGTTGAAGGTAGTTTCGTG